Article

Polyethylene/Bacterial-Cellulose Biocomposite Synthesized via In Situ Polymerization with Zirconocene/MMAO Catalyst

Natthadabhorn Thanarattanasap[1,a], Praonapa Tumawong[1], Thipprapa Sinsawat[1], Ekrachan Chaichana[2,b,*], and Bunjerd Jongsomjit[1,c]

1 Center of Excellence on Catalysis and Catalytic Reaction Engineering, Department of Chemical Engineering, Faculty of Engineering, ChulalongkornUniversity, Bangkok 10330, Thailand
2 Research Center of Natural Materials and Products, Chemistry Program, Faculty of Science and Technology, Nakhon Pathom Rajabhat University, Muang, Nakhon Pathom 73000, Thailand
E-mail: [a]bewviezz@gmail.com, [b]ekrachan@yahoo.com (Corresponding author), [c]bunjerd.j@chula.ac.th

Abstract. In this study, the polyethylene filled celluloses regarded as biocomposites was produced via in situ polymerization with zirconocene/MMAO catalyst. Three types of celluloses including microcrystalline cellulose (MCC), bacterial cellulose prepared from pineapple shell extract (BCP), and bacterial cellulose prepared from coconut (BCC) were used as fillers and also catalytic support in the polymerization system. It was found that the presence of cellulose fillers slightly decreased catalytic activity of the polymerization system, but it was still higher compared with that of other natural fillers such as coir dust. This is caused by the lower impurity of cellulose. The MCC provided the highest catalytic activity among all cellulose fillers. The obtained biocomposites were characterized with different techniques including scanning electron microscope (SEM) and thermal gravimetric analysis (TGA). It was observed that all obtained biocomposites exhibited good morphology compared with the neat polyethylene. Thermal stability of the polymers was improved with the cellulose fillers.

Keywords: Polyethylene, metallocene, cellulose, biocomposite.

1. Introduction

Polyethylene (PE) is the most widely used polymer in packages and is available in a variety of densities: low density (LDPE), linear low density (LLDPE), medium density (MDPE), and high density (HDPE) [1]. It is also used to produce water pipe, toys, foam, geomembranes, bulletproof vests, etc. due to its unique properties such as light weight, high chemical resistance, and low dielectric constant. There is a forecast that global demand for polyethylene resins will rise 4% per year to 99.6 million metric tons in 2018, valued at $164 billion [2]. This could lead to serious environmental problems since biodegradation of commercial high molecular weight polyethylene proceeds slowly. In order to enhance environmental degradability to polyethylene, it must be blended with biodegradable additives or photo-initiators [3]. Blending or addition of natural fillers like palm leaf [4], guayule biomass [5], banana stem fiber [6], grass fiber [7], and coconut shell powder [8] into polymer matrices has been studied and exhibits biodegradability besides of renewability, low cost and low density and so on [9]. However, the main drawback of introducing the natural fillers into the synthetic polymer is the poor compatibility between the natural fillers and the polymer matrix and the poor distribution of the natural fillers throughout the polymer matrix, due mainly to the different polarities between two phases. This causes the polymer biocomposites to have undesirable properties. In fact, there are about three methods used to produce the filled polymer; (i) melt mixing, (ii) solution blending, and (iii) *in situ* polymerization [10]. Due to the direct synthesis via polymerization along with the presence of the natural filler, the *in situ* polymerization may be an efficient technique to produce polymer biocomposite with good compatibility and good distribution of the natural fillers.

Previously, the polyethylene/coir-dust biocomposite is produced via the in situ polymerization with zirconocene/MAO (methylaluminoxane) catalyst by our group [11]. It is found that the polyethylene biocomposites can be produced with this method. Nevertheless, the catalytic activity of the polymerization system with the presence of coir dust filler is lower than the one without the coir dust. This is due to the higher content of impurities inside the coir dust especially the amine compound as seen from FT-IR analysis (primary amine, $-NH_2$) which possibly leads to the deactivation of the zirconocene catalyst. To overcome this problem, higher purity natural fillers should be used instead. Bacterial cellulose (BC) obtainable through fermentation is considered nearly pure cellulose [12]. In addition, BC attracts extensive attention due to its unique properties, such as its high degree of polymerization, good biocompatibility, biodegradability, high crystallinity and excellent mechanical properties [13]. Therefore, BC could be potentially used as a natural filler in the in situ polymerization system to produce polyethylene biocomposite. Saowapark *et al.* [14] used BC as a filler in rubber composite and found that it enhanced most mechanical properties to the obtained composite including tensile strength, tensile modulus and tear strength.

In this study, the *in situ* polymerization of ethylene along with BC filler can be carried out by supporting cocatalyst (MMAO) onto BC, then bringing it into the polymerization system along with the metallocene catalyst, and finally polyethylene biocomposite filled with BC was obtained. Two kinds of bacterial cellulose prepared from pineapple shell extract and coconut water were used here. In addition, commercial microcrystalline cellulose was also used in the study to compare with the BC. The catalytic activity of the polymerization systems and the characteristic of the biocomposite products were investigated using an X-ray diffraction analysis (XRD), differential scanning calorimeter (DSC), scanning electron microscope (SEM) and thermal gravimetric analysis (TGA).

2. Experimental

2.1. Materials

Ethylene gas (99.99%) was donated by National Petrochemical Co., Ltd. Thailand. Modified methylaluminoxane (MMAO) was supplied by Tosoh Finechem, Co., Ltd. Japan. The *rac*-ethylenebis(indenyl)zirconium dichloride [Et(Ind)$_2$ZrCl$_2$] was supplied by Sigma-Aldrich (Thailand). Bacterial celluloses were prepared as described in Section 2.2. Microcrystalline cellulose (Avicel PH 101) was supplied from FMC Chemical (Thailand) Ltd. Toluene was devoted from ExxonMobil Chemical (Thailand) Ltd. Ultra high purity argon gas (99.999%) was purchased from Thai Industrial Gas Co., Ltd. Thailand. Hydrochloric acid (Fuming 36.7%) was supplied from Sigma-Aldrich (Thailand) Co., Ltd. Methanol (commercial grade) was purchased from SR lab, Thailand.

2.2. Preparation of Bacterial Cellulose

For preparation of bacterial cellulose through fermentation, pineapple shell extract and coconut water were used as carbon sources. The fermentation was conducted with using bacteria, namely Acetobacter xylinum (TISTR 975) in culture media solution composing of pineapple shell extract or coconut water, ammonium sulfate ((NH_4)$_2SO_4$), sucrose ($C_{12}H_{22}O_{11}$) and acetic acid (CH_3COOH). The mixture was incubated for 1 week at 28°C. After that, the bacterial cellulose sheet (1.5 mm of thickness) was obtained, then washed in 0.5 M NaOH at 70°C in order to remove bacteria, and neutralized with water.

2.3. Preparation of Cellulose Filler

All celluloses were immobilized with MMAO, acting as catalytic support in the polymerization system and simultaneously as a filler in the obtained polymer. The celluloses were calcined under vacuum at 150°C for 4 h with a heating rate of 10°C/min prior to immobilization. The desired amount of cellulose (0.5 g) and 5 mL of MMAO were mixed and stirred for 30 min aging at room temperature. Then, the mixture was vacuum dried at room temperature and the solid powder of cellulose/MMAO was obtained.

2.4. In situ Polymerization

Ethylene polymerization reaction was operated in 100 ml semi-batch stainless steel autoclave reactor with magnetic stirrer. Approximately, 0.2 g of cellulose/MMAO filler was added into the reactor followed by 1.5 mL of Et(Ind)$_2$ZrCl$_2$ (5×10^{-5} M). Toluene was added into the reactor to fill a total volume of reactor as 30 mL at room temperature. The reactor was heated up to polymerization temperature (70°C) and the mixture was stirred during heating up. When reached 70°C, ethylene was fed into the reactor under pressure of 3.5 bar for 15 minutes. The obtained slurry was added of acidic methanol (0.1% HCl in methanol) and stirred overnight. Finally, a wet polymer was separated by filtered, and was washed using methanol and dried at room temperature.

2.5. Characterization

2.5.1. Scanning electron microscope (SEM)

The morphology of cellulose before and after immobilization with MMAO was investigated by using JEOL mode JSM-6400 model of SEM. The sample was conductive to prevent charging by coating with gold particle by ion 45 sputtering device.

2.5.2. X-ray diffraction (XRD)

To investigate bulk crystalline phases of cellulose materials, the XRD was used in the 2θ range of 10 to 80 degrees using SIEMENS D-5000 X-ray diffractometer with CuKα radiation (λ = 1.54439×10^{-10} m) with Ni filter. The spectrum rate was scanned at 2.4 degree/min.

2.5.3. Thermal gravimetric analysis (TGA)

Thermal stability of cellulose materials and obtained polymers was determined using the TGA instrument by TA Instruments SDT Q600 analyzer.

2.5.4. Differential scanning calorimetry (DSC)

The DSC, DSC 204 F1 Phoenix®, was used to measure melting temperature (T_m) and crystallinity (X_c) of the polymers. Approximately, 10-20 mg of sample was used. Carrier gas was nitrogen UHP. The temperature ramp was operated from 25 to 700°C at 10°C/min.

3. Results and Discussion

3.1. Characterization of Cellulose

Two kinds of bacterial cellulose from pineapple shell extract and coconut water designated as BCP and BCC, and microcrystalline cellulose (commercial) as MCC were first characterized with various techniques prior immobilization with MMAO. The morphologies of the cellulose obtained with SEM are shown in Fig. 1. It can be seen that both bacterial cellulose (BCP and BCC) displayed rough surface with a few fibers present, whereas MCC exibited flake-like structure with a smoother surface. Particle sizes of MC were significantly smaller than those of both BC which had particle sizes of 100-300 μm.
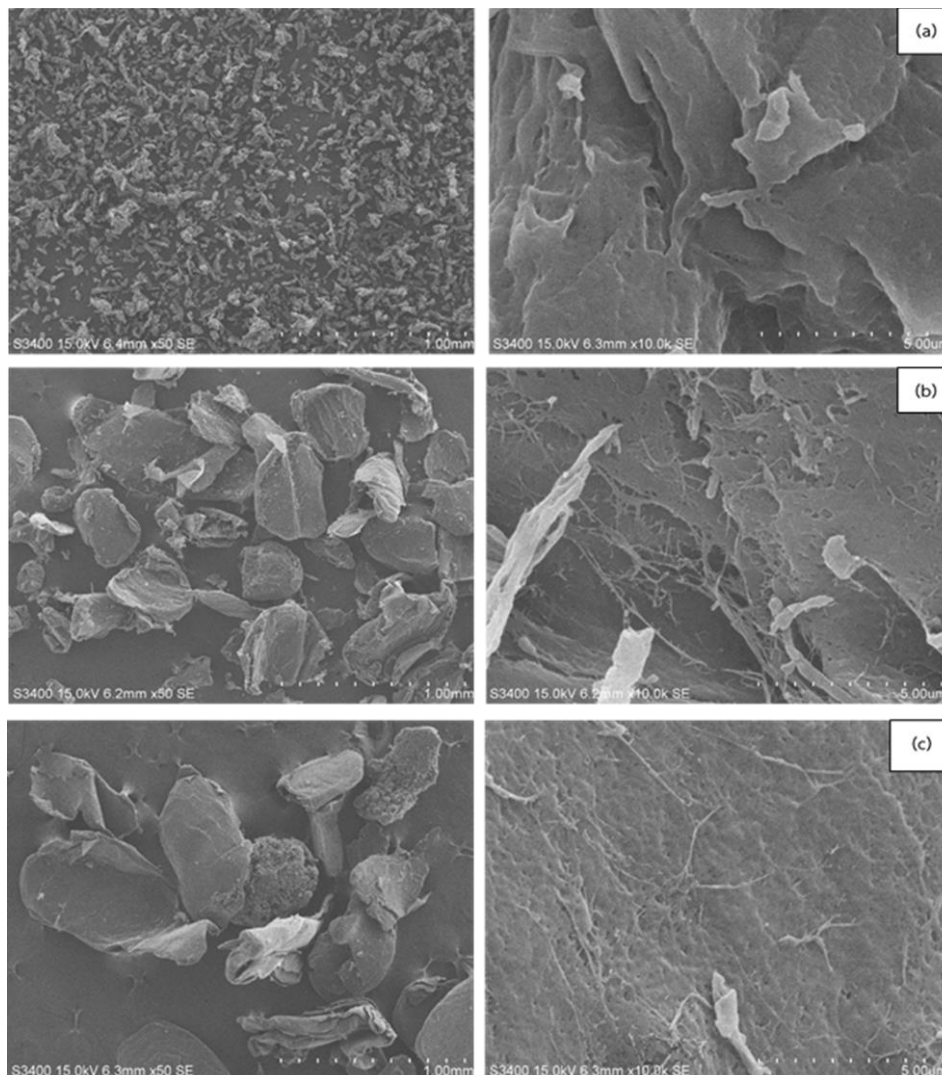

Fig. 1.   Morphologies of celluloses: (a) MCC, (b) BCP and (c) BCC.

Crystal structures of the cellulose were investigated by X-ray diffraction (XRD) as shown in Fig. 2. The XRD patterns of all cellulose samples were similar, presenting the characteristic peaks at 2θ equal to 14.8, 16.2, 22.5, and 34.5, which were assigned to the typical cellulose crystalline form [15]. It was also observed that BCP exhibited the shaper peaks at 2θ equal to 14.8 and 16.2 compared to the other two samples. This probably indicates the higher extent of crystallinity and larger crystallite size of BCP than the others.
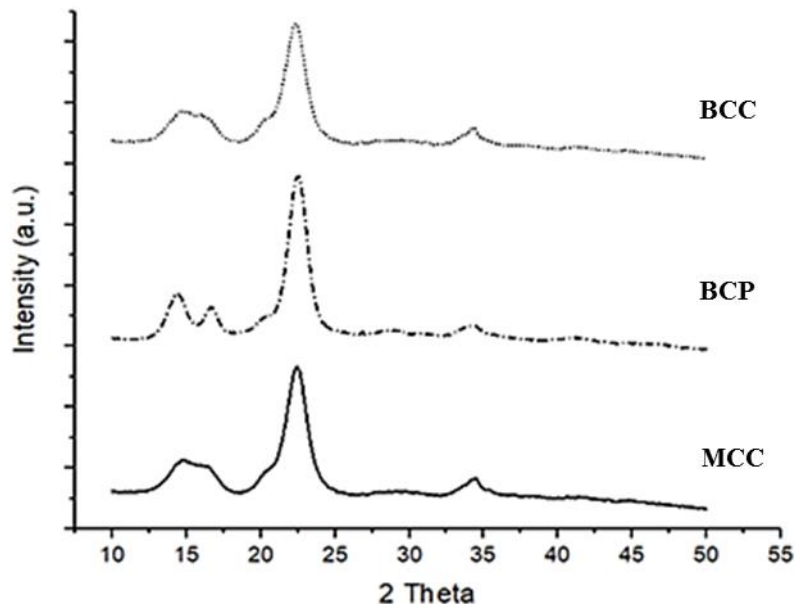
Fig. 2.   XRD patterns of celluloses.

The FT-IR spectra of the cellulose are shown in Fig. 3. It can be seen that all cellulose exhibited the similar FTIR spectra with broad bands around 3331-3337 cm^{-1} corresponding to stretching vibration of the boned hydroxyl group. The peak at 1446 cm^{-1} was assigned to the symmetry of CH$_2$ bending vibration. The sharp peak of percentage of transmittance at range of 1026-1020 cm^{-1} was corresponded to strong bond of C-C, C-OH, and C-H group vibration [16]. The alcohol functional groups were also observed in all celluloses indicating the O-H stretching at 3000-2780 cm^{-1}, C-H stretching at 1500-1300 cm^{-1}, and C-O stretching at 1100 cm^{-1}[17].
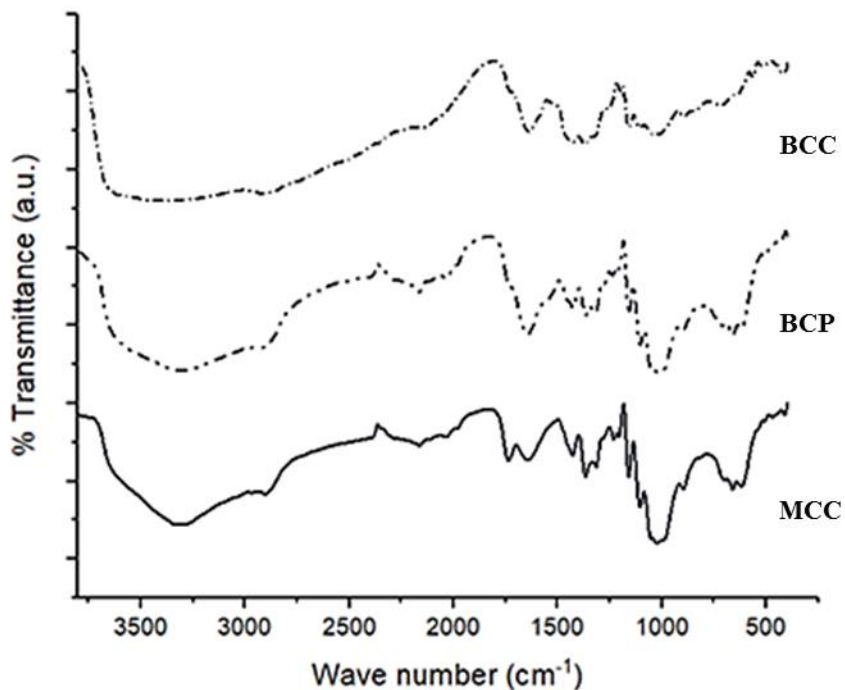

Fig. 3.   FTIR spectra of cellulose.

3.2. Characterization of Cellulose/MMAO Filler

After MMAO was immobilized on the celluloses, the finished filler (cellulose/MMAO) was investigated for changes in morphology and crystalline structures, and also the distribution of MMAO on the filler surface. The morphologies of the fillers are shown in Fig. 4. It can be seen that all fillers exhibited the significantly different morphologies compared to the pristine celluloses due to the presence of the MMAO on their surface. The agglomerated particles were observed in all fillers.

To examine the distribution of MMAO on the filler surfaces, the SEM/EDX techniques were employed. EDX provided the location of Al element (represented as dots) related to the existence of MMAO on the filler surfaces as seen in Fig. 5. It was observed that the MMAO was well distributed all over the filler surfaces in all cellulose types.
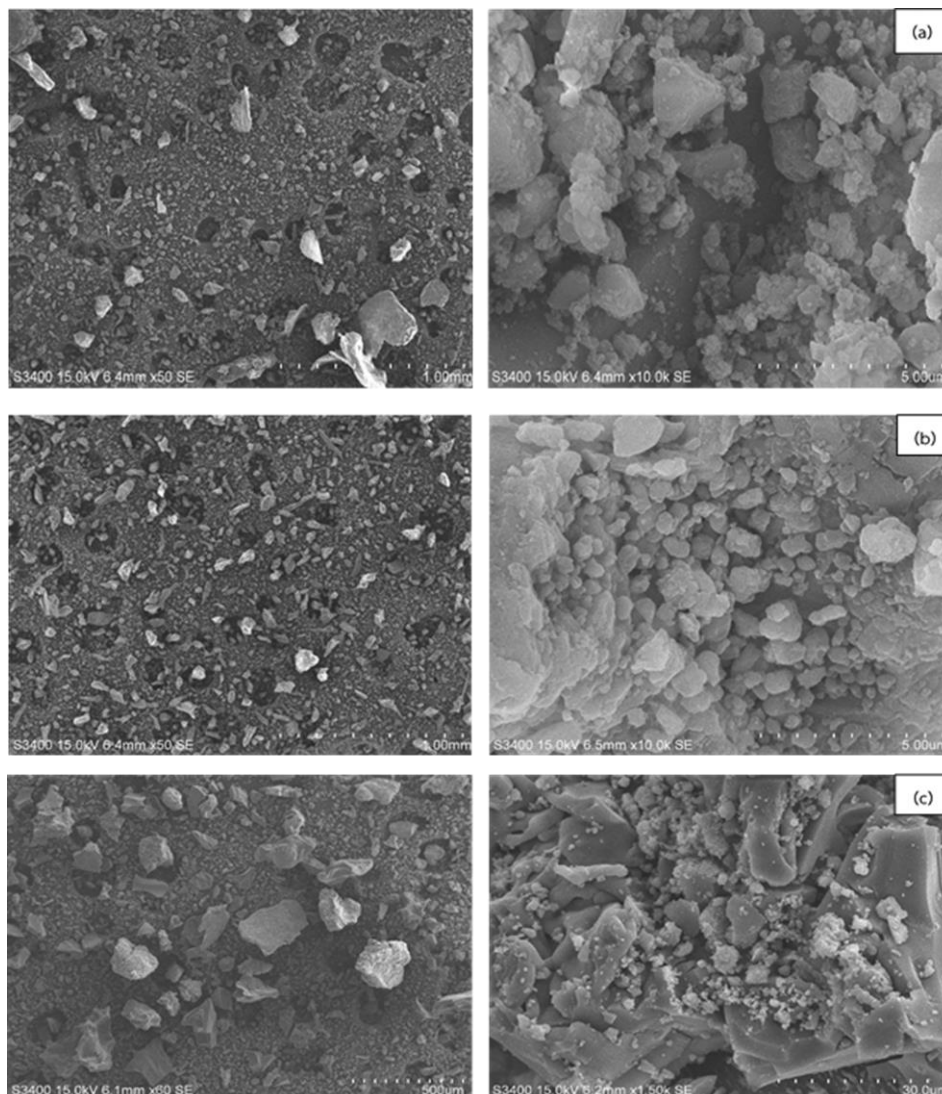

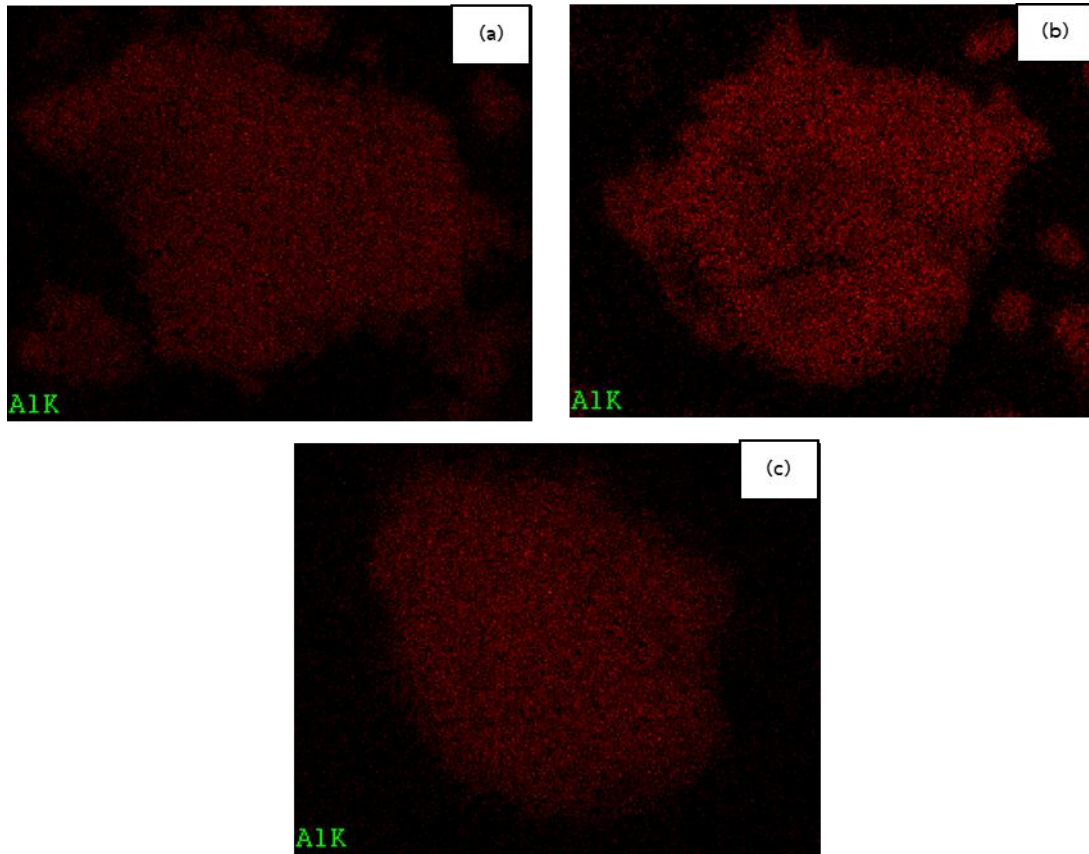Fig. 4. SEM micrographs of cellulose fillers: (a) MCC/MMAO, (b) BCP/MMAO and (c) BCC/MMAO.

Fig. 5.   Al distribution on cellulose fillers: (a) MCC/MMAO, (b) BCP/MMAO and (c) BCC/MMAO.

Crystal structures of the fillers were also determined with the XRD as shown in Fig. 6. The slight changes in the XRD peaks were observed for all fillers as seen that the broader XRD peaks compared to those of the pristine cellulose appeared. This is probably due to lower crystallinity of the filler after immobilization. BCC/MMAO filler exhibited some characteristic peaks of cellulose. This was probably because the MMAO did not cover the entire surface of BCC. Nevertheless, no distinct peaks attributed to Al atom (MMAO) were observed in the XRD patterns of all fillers suggesting to highly dispersed form of MMAO onto the filler surfaces.
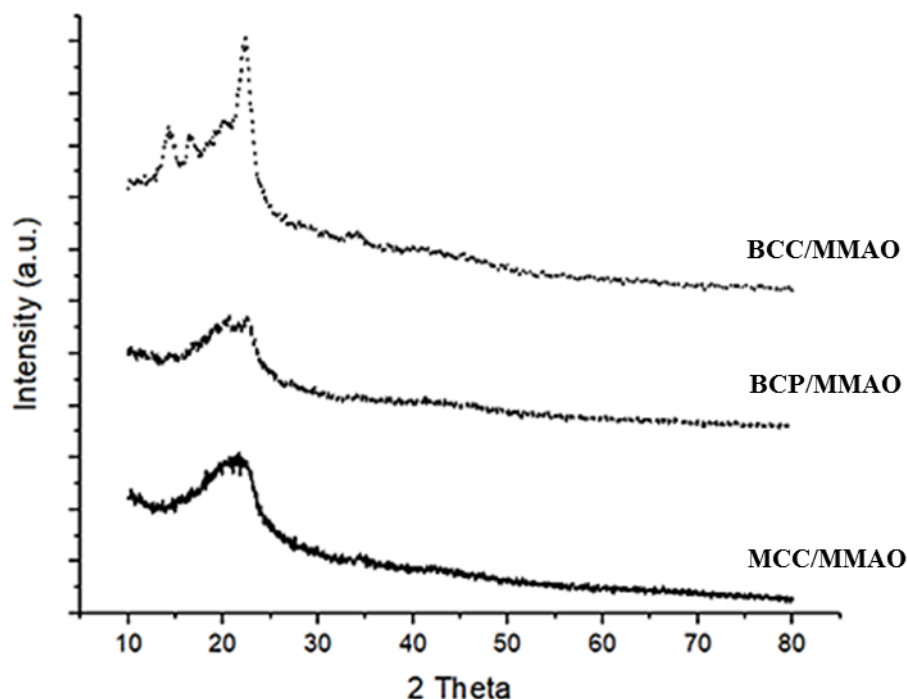
Fig. 6. XRD patterns of cellulose fillers.

It was due to the cellulose fillers here also exhibited a role as catalytic supports for the MMAO, which was a cocatalyst in the polymerization. The amount of MMAO on the filler surface and the interaction between them are crucial factors influencing the catalytic system. Those factors can be determined using an X-ray photoelectron spectroscopy (XPS), and the obtained results from the XPS technique are shown in Table 1. The binding energy (BE) of Al in orbital 2p core level of Al atom on various fillers were between 74.7 and 75.8 eV nearly to that of Al atom in the pure MMAO. A slight shift in BE value of $Al_{[MMAO]}$ in the fillers was resulted from the interaction of MMAO and the filler surface. The amounts of $Al_{[MMAO]}$ on MCC and BCC were higher than that of the pure MMAO, while the opposite was true for BCP. It worth noting that the XPS is a a highly sensitive surface analysis method with analysis depth approximately 5 nm. Thus, the rougness of the sample could alter the XPS result as seen that the amounts of Al atom at surface of the fillers with immobilized MMAO were even higher than that of the actual MMAO. Nevertheless, comparing among all fillers, the XPS result indicates that MMC and BCC had the amounts of MMAO at the surface signicantly higher than that of BCP. This contrasted with the amounts of MMAO in bulk, which were quantified by ICP technique as also shown in Table 1. It was in the order of BCC > BCP > MCC. This suggests that the fillers had various amounts of MMAO located at different depths. Particularly, BCC had the MMAO mostly located at the surface, even having the lowest amount of it among all fillers.

Table 1. Characteristics of Al in MMAO obtained from XPS and ICP of various cellulose/MMAO fillers.

Samples	Binding Energy of Al (eV)[a]	Amount of Al at surface (%wt.)[a]	Amount of Al in bulk (%wt.)[b]
MMAO [18]	74.7	28.50	-
MCC/MMAO	75.6	34.76	19.71
BCP/MMAO	75.8	23.48	22.54
BCC/MMAO	74.7	35.38	23.63

[a]Obtained from XPS.
[b]Obtained from ICP.

3.3. *In situ* Polymerization

All finished cellulose/MMAO fillers were introduced into polymer (polyethylene) through the *in situ* polymerization with the zirconocene catalyst to obtain the polyethylene biocomposites. Due to the fillers being introduced during the polymerization, the variation in catalytic activity of the polymerization system deriving from the presence of the fillers need to be concerned. The catalytic activity of each polymerization system was calculated from their polymerization time and the polymer yield, which are shown in Table 2. The polymerization systems are classified into two types i.e. homogeneous: without the filler or the catalyst support, and heterogeneous: with the presence of fillers. It was seen that the homogeneous system still exhibited higher catalytic activity than those of all heterogeneous systems. This was due to negative supporting effects from the presence of the cellulose fillers in the polymerization system [19]. The fillers could prevent the access of the ethylene monomer into the catalytically active sites, and the interaction between the catalytically active sites and the cellulose surface may reduce the reactivity of the catalysts toward the monomer. However, when comparing the cellulose fillers in this study and the coir dust in our previous study, it was found that the presence of cellulose fillers in this study apparently decreased the catalytic activity about 1.1 times of the homogeneous system, while the coir dust with the best condition decreased the catalytic activity up to 1.8 times [11]. This could be resulted from the high impurity of the celluloses in this study according to our assumption above. Considering on the heterogeneous systems with the cellulose, it was found that all systems can be conducted successfully without any faults. This exhibits a practical way to produce polymer biocomposites through the *in situ* polymeization with the zirconocene/MMAO catalyst.

The catalytic activity of MMC was the highest among all fillers. This was problably due to the smallest particle size among all celluloses. The smaller particle size has less diffusion resistance, and more surface area resulting in the good distribution of the catalytically active sites on the particle [20]. For the bacterial celluloses, BBC exbibited higher catalytic activity than BCP. This agrees with the amount of MMAO on both bacterial celluloses as observed with the XPS and ICP techniques. In addition, it can be observed that the catalytic acitivities tend to be consistent with the amount of MMAO at the surface of the filler than that in the bulk. This suggests that the MMAO at the surface is more crucial in the metallocene catalytic system.

Table 2.   Catalytic activities of the *in situ* polymerization with different cellulose fillers.

System	Fillers	Polymerization yield[a] (g)	Catalytic activity[b] (kg of pol/molZr h)
Homogeneous	-	0.6861	331
Heterogeneous	MCC	0.6183	298
	BCP	0.5288	255
	BCC	0.5630	271

[a] The polymerization time was 15 min.

[b] Activities were measured at polymerization temperature of 70 $^\circ$C, [ethylene] = 0.018 mole, $[Al]_{MMAO}/[Zr]_{cat}$ = 1135, in toluene with total volume = 30 mL, and $[Zr]_{cat}$ = 5 x 10^{-5} M.

3.4. Characterization of polymers

The obtained biocomposites (PE/celluloses) and the neat polyethylene (PE) were characterized for morphology using the SEM, as shown in Fig. 7. It shows that PE exhibited a spongy-like structure with low packed density, clearly differed from all biocomposites. It was observed that the polymer particles developed in the biocomposites due to the presence of the cellulose fillers in the polymerization system. This leads to good polymer morphology. The polymer with particle-like structure and a low amount of fine particles decreases reactor fouling during polymerization and makes the polymers easily handle during processing [19]. Producing polymers with good morphology is considered an advantage of the heterogeneous system with the fillers over the homogeneous one. For all biocomposites, PE/BCP possed the larger particles than PE/MCC and PE/BCC, which had nearly similar size.
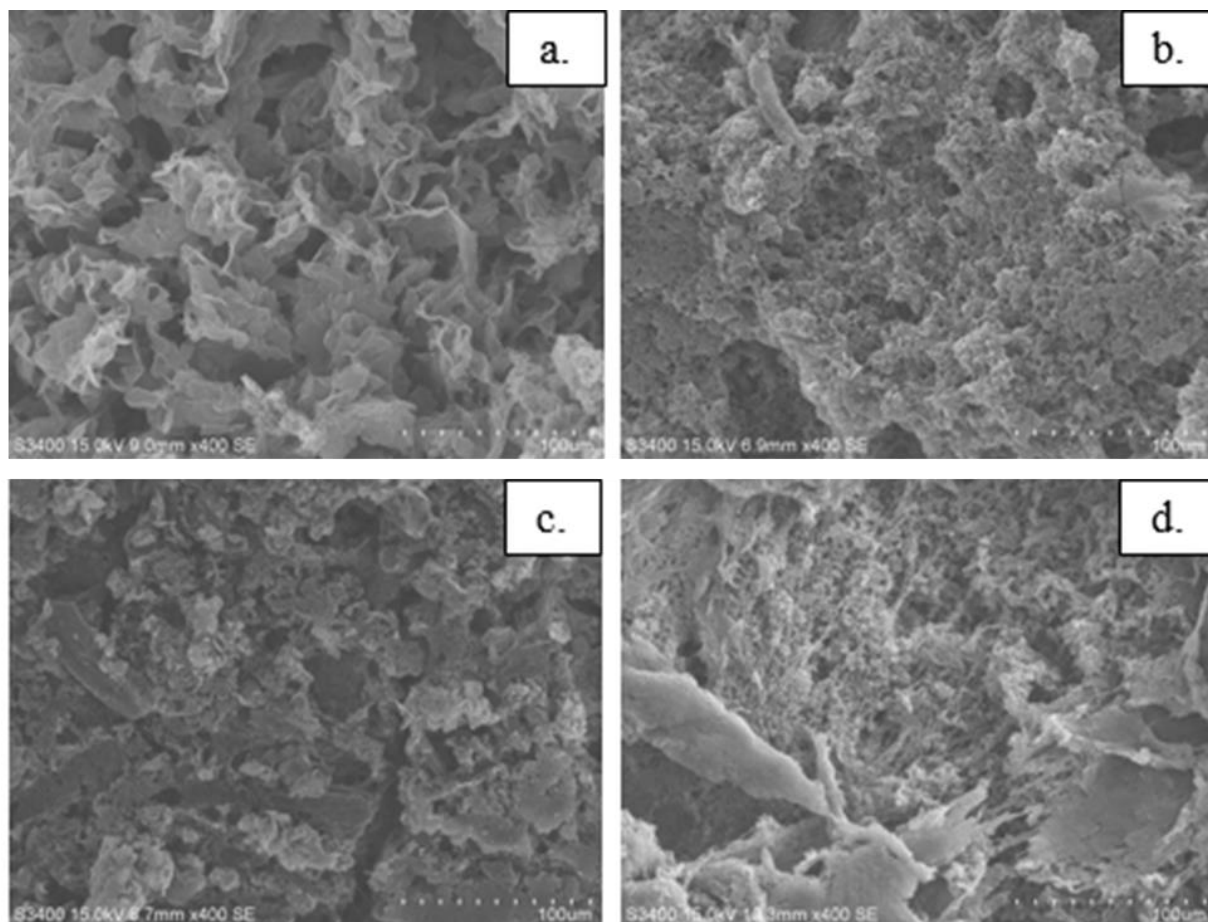
Fig. 7.   The morphologies of polymers; (a) PE (b) PE/MCC, (c) PE/BCP and (d) PE/BCC.

All polymer samples were identified for their crystal structure using the XRD analysis, and the XRD patterns of the polymers are shown in Fig. 8. It was observed that all polymers exhibited the similar sharp peaks at 21.5° and 23.9°, which are characteristic peaks of typical ethylene [21]. This suggests that the cellulose fillers could produce polyethylene biocomposites with the same crystal structure as typical polyethylene. In addition, there was no difference of crystal structure among all biocomposites obtained from various fillers.
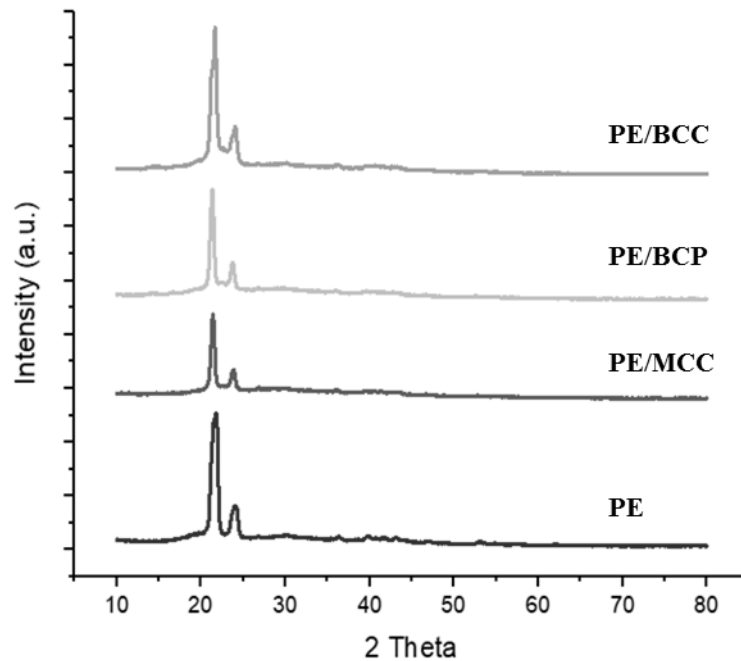
Fig. 8.   XRD patterns of polymers produced from various systems.

Thermal properties of the polymers including melting temperature (T_m), crystallization enthalpy (ΔH_{exp}) and crystallinity (X_c) were investigated using the DSC measurement, as shown in Table 3. Melting temperatures of all samples were close ranging between 122 and 124°C, within a normal range of polyethylene melting temperature (115–135°C). Various fillers did not affect melting temperature of the obtained polymers. Nevertheless, crystallinity of the polymers varied with the fillers. It was observed that the crystallinity values of biocomposites with bacterial celluloses (PE/BCP and PE/BCC) were higher than those of the one with microcrystalline cellulose (PE/MCC) and also the neat polyethylene (PE). This suggests that the bacterial celluloses increase crystallinity to the polymer probably because it acts as heterophase crystal nucleation agent in the polymer matrix [22]. This case was not observed for microcrystalline cellulose. It may be concluded that the different types of celluloses cause different effect on the crystallization process of polymers and consequently lead to the different crystallinity of polymers.

Table 3.   Thermal properties of polymers produced from various systems.

Samples	Melting Temperature T_m (°c)	Heat of fusion ΔH_{exp} (J/g)	Crystallinity X_c[a] (%)
PE	124	164.4	57.5
PE/MCC	122	167.2	58.5
PE/BCP	123	215.9	75.5
PE/BCC	122	209.5	73.2

[a]$X_c = \Delta H_{sample}/\Delta H_{100\%}$ crystallinity (286 J/g) x 100

Thermal stability of the polymers was determined using the TGA technique which displays the degree of thermal stability by measuring the weight loss of a sample as a function of temperature. The TGA profiles of the polymers (Fig. 9.) shows that both biocomposites with BC (PE/BCP and PE/BCC) exhibited the characteristic curves of thermal stability differed from PE and PE/MCC. From the differential thermal analysis (DTA) profiles in Fig. 10., it clearly indicated losing of absorbed moisture around 100°C for PE and PE/MCC but not for PE/BCP and PE/BCC which gradual changes of weight loss at this temperature were observed instead. The presence of BC may interrupt moisture evaporation process in the polymer. For all

biocomposites, they exhibited the notable weight loss around 250-350°C, resulting from dehydration and decomposition of the cellulose [23]. However, an early stage of cellulose decomposition did not adversely affect the thermal stability of the polymers. It was observed that the maximum decomposition temperature (the highest change in weight loss) of all polymers were narrow; between 476 and 481°C. The addition of cellulose fillers slightly increased the maximum decomposition temperature to the polymers as follows; PE/MCC (481°C) > PE/BCP (480°C) = PE/BCC (480°C) > PE (476°C). From this trend, raising the amount of cellulose into the polymer may increase the maximum decomposition temperature or thermal stability of the polymers. Huq *et al.* [24] have also found from the TGA result that addition of cellulose (nanocrystalline) into films makes TGA curves shifted toward higher temperatures, suggesting better thermal stability of cellulose reinforced films.
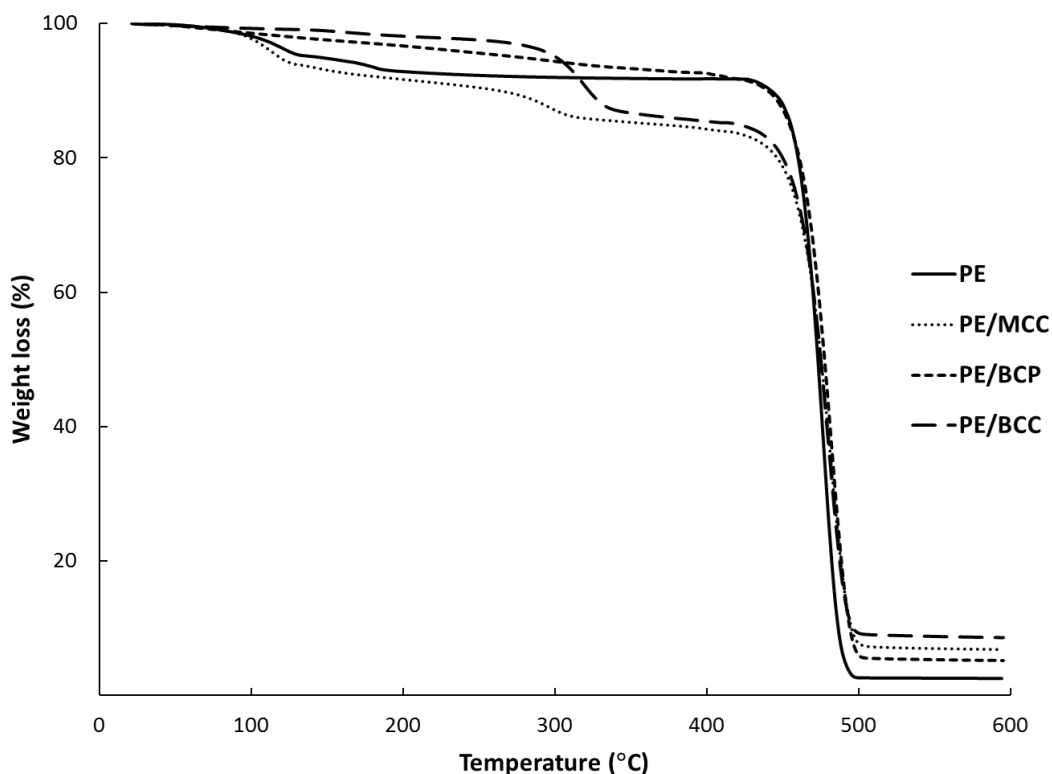

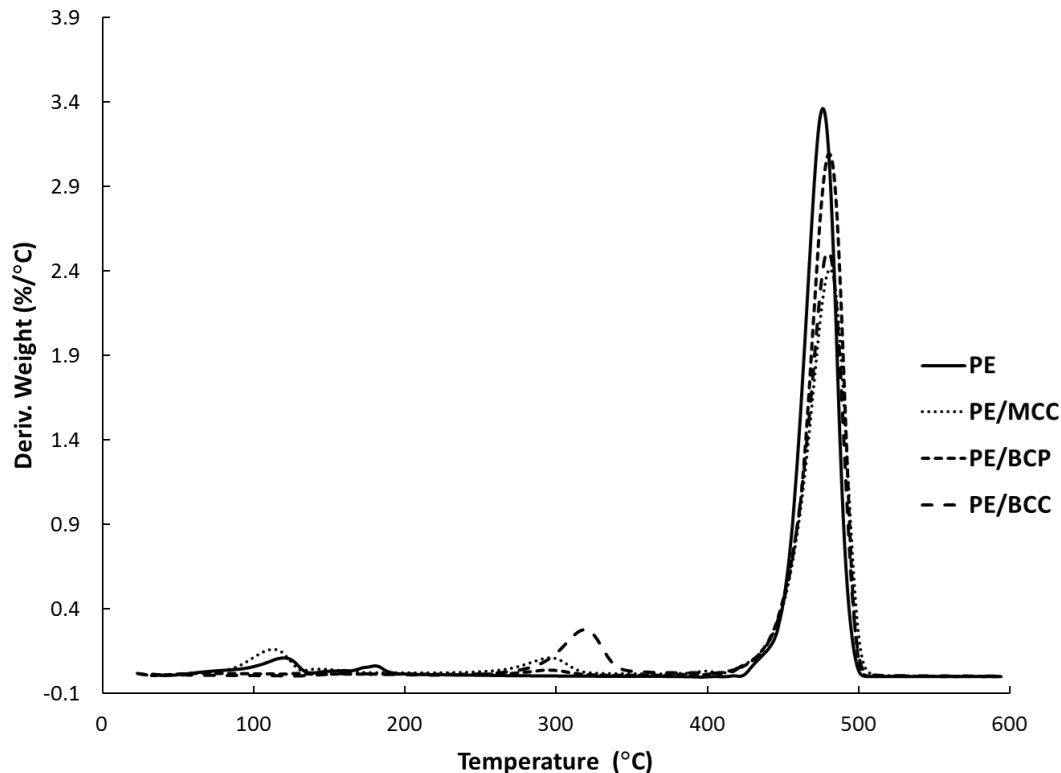Fig. 9.   TGA profiles of polymers produced from various systems.

Fig. 10. DTA profiles of polymers produced from various systems.

4. Conclusion

Three types of celluloses: MCC, BCP and BCC were used as fillers for production of polyethylene via *in situ* polymerization with zirconocene/MMAO catalyst. It was found that the polyethylene filled celluloses regarded as biocomposites was completely achieved through this method. The presence of cellulose fillers slightly decreased catalytic activity of the polymerization system, but it was still higher compared with that of other natural fillers such as coir dust. This was due to the lower impurity of cellulose. The MCC provided the highest catalytic activity among all cellulose fillers. All obtained biocomposites exhibited good morphology compared with the neat polyethylene. Thermal stability of the polymers was also improved with the cellulose fillers.

Acknowledgement

References

[1]   L. Mauer and B. Caballero, "PACKAGING | Aseptic Filling," in *Encyclopedia of Food Sciences and Nutrition*, 2nd ed. Oxford: Academic Press, 2003, pp. 4316-4322.
[2]   "Global demand for polyethylene to reach 99.6 million tons in 2018," *Pipeline Gas J.*, vol. 241, no. 12, p. 52, 2014.
[3]   S. Bonhomme, A. Cuer, A. M. Delort, J. Lemaire, M. Sancelme, and G. Scott, "Environmental biodegradation of polyethylene," *Polym. Degrad. Stab.*, vol. 81, no. 3, pp. 441-452, 2003.

[4] M. A. Binhussain and M. M. El-Tonsy, "Palm leave and plastic waste wood composite for out-door structures," *Constr. Build. Mater.*, vol. 47, pp. 1431-1435, 2013.

[5] S. G. Bajwa, D. S. Bajwa, G. Holt, T. Coffelt, and F. Nakayama, "Properties of thermoplastic composites with cotton and guayule biomass residues as fiber fillers," *Ind. Crops Prod.*, vol. 33, no. 3, pp. 747-755, 2011.

[6] I. C. Ezema, A. R. Menon, C. S. Obayi, and A. D. Omah, "Effect of surface treatment and fiber orientation on the tensile and morphological properties of banana stem fiber reinforced natural rubber composite," *J. Miner. Mater. Charact. Eng.*, vol. 2, pp. 216-222, 2014.

[7] D. De, D. De, and B. Adhikari, "The effect of grass fiber filler on curing characteristics and mechanical properties of natural rubber," *Polym. Adv. Technol.*, vol. 15, no. 12, pp. 708-715, 2004.

[8] T. V. Jinitha, M. P. Sreejith, A. K. Balan, and E. Purushothaman, "Mechanical and transport properties of permanganate treated coconut shell powder–natural rubber composites," *J. Chem. Pharm. Sci.,* vol. 1, pp. 5-11, 2016.

[9] N. Dinh Vu, H. Thi Tran, and T. Duy Nguyen, "Characterization of polypropylene green composites reinforced by cellulose fibers extracted from rice straw," *Int. J. Polym. Sci.*, p. 10, 2018.

[10] E. Chaichana, B. Jongsomjit, and P. Praserthdam, "Effect of nano-SiO$_2$ particle size on the formation of LLDPE/SiO$_2$ nanocomposite synthesized via the in situ polymerization with metallocene catalyst," *Chem. Eng. Sci.*, vol. 62, no. 3, pp. 899-905, 2007.

[11] C. Suttivutnarubet, A. Jaturapiree, E. Chaichana, P. Praserthdam, and B. Jongsomjit, "Synthesis of polyethylene/coir dust hybrid filler via in situ polymerization with zirconocene/MAO catalyst for use in natural rubber biocomposites," *Iran. Polym. J.*, vol. 25, no. 10, pp. 841-848, 2016.

[12] N. Kanjanamosit, C. Muangnapoh, and M. Phisalaphong, "Biosynthesis and characterization of bacteria cellulose-alginate film," *J. Appl. Polym. Sci.*, vol. 115, no. 3, pp. 1581-1588, 2010.

[13] V. Revin, E. Liyaskina, M. Nazarkina, A. Bogatyreva, and M. Shchankin, "Cost-effective production of bacterial cellulose using acidic food industry by-products," *Braz. J. Microbiol.*, vol. 49, pp. 151-159, 2018.

[14] T. Saowapark, E. Chaichana, and A. Jaturapiree, "Properties of natural rubber latex filled with bacterial cellulose produced from pineapple peels," *J. Met. Mater. Miner.*, vol. 27, no. 2, pp. 12-16, 2017.

[15] S. Park, J. O. Baker, M. E. Himmel, P. A. Parilla, and D. K. Johnson, "Cellulose crystallinity index: Measurement techniques and their impact on interpreting cellulase performance," *Biotechnol. Biofuels*, vol. 3, no. 1, pp. 10, 2010.

[16] M. Fan, D. Dai, and B. Huang, "Fourier transform infrared spectroscopy for natural fibres," in *Fourier Transform – Materials Analysis*, S. Salih, Ed. London: IntechOpen Limited, 2012.

[17] D. N. T. Magalhães, O. Do Coutto Filho, and F. M. B. Coutinho, "Ziegler-natta catalyst for ethylene and propylene polymerization supported on adducts of magnesium chloride with methyl and ethyl alcohols," *Eur. Polym. J.*, vol. 27, no. 8, pp. 827-830, 1991.

[18] C. Ketloy, B. Jongsomjit, and P. Praserthdam, "Characteristics and catalytic properties of [t-BuNSiMe$_2$Flu] TiMe$_2$/dMMAO catalyst dispersed on various supports towards ethylene/1-octene copolymerization," *Appl. Catal., A*, vol. 327, no. 2, pp. 270-277, 2007.

[19] G. G. Hlatky, "Heterogeneous single-site catalysts for olefin polymerization," *Chem. Rev.*, vol. 100, no. 4, pp. 1347-1376, 2000.

[20] E. Chaichana, P. Rothakit, P. Praserthdam, and B. Jongsomjit, "PE and LLDPE/spherical-silica composite synthesized via in situ polymerization with zirconocene/MAO catalyst," *J. Thai Interdiscip. Res.*, vol. 11, no. 2, pp. 29-41, 2016.

[21] K. E. Russell, B. K. Hunter, and R. D. Heyding, "Monoclinic polyethylene revisited," *Polym.*, vol. 38, no. 6, pp. 1409-1414, 1997.

[22] X. Wang, T. T. Fangfang, X. Gi, J. Zhu, T. Chen, P. Sun, H. H. Winter, and A.-C. Shi, "Enhanced exfoliation of organoclay in partially end-Functionalized non-polar polymer," *Macromol. Mater. Eng.*, vol. 294, no. 3, pp. 190-195, 2009.

[23] C. Y. Lee, M. U. Wahit, and N. Othman, "Thermal and flexural properties of regenerated cellulose(rc)/poly(3- hydroxybutyrate)(phb)biocomposites," *J. Teknol.*, vol. 75, no. 11, pp. 107-112, 2015.

[24] T. Huq, S. Salmieri, A. Khan, R. A. Khan, C. Le Tien, B. Riedl, C. Fraschini, J. Bouchard, J. Uribe-Calderon, M. R. Kamal, and M. Lacroix, "Nanocrystalline cellulose (NCC) reinforced alginate based biodegradable nanocomposite film," *Carbohydr. Polym.*, vol. 90, no. 4, pp. 1757-1763, 2012.